Valtonen Anu (Orcid ID: 0000-0003-1532-1563)

Remotely-sensed vegetation greening along a restoration gradient of a tropical forest, Kibale National Park, Uganda

Anu Valtonen[1,*], Eveliina Korkiatupa[1], Sille Holm[1,2], Geoffrey M. Malinga[1,3], Ryosuke Nakadai[1,4,5]

[1]Department of Environmental and Biological Sciences, University of Eastern Finland, P.O. Box 111, 80101 Joensuu, Finland

[2]Department of Zoology, Institute of Ecology and Earth Sciences, University of Tartu, Vanemuise 46, EE-51014 Tartu, Estonia

[3]Department of Biology, Gulu University, P.O. Box 166, Gulu, Uganda

[4]Graduate School of Agricultural and Life Sciences, The University of Tokyo, 1-1-1 Yayoi, Bunkyo-ku, Tokyo 113-8657, Japan

[5]Biodiversity Division, National Institute for Environmental Studies, Onogawa 16-2, Tsukuba, Ibaraki, 305-8506, Japan

*Corresponding author: Anu Valtonen, E-mail: anu.valtonen@uef.fi

A short informative containing the major key words: This work assesses 20 years of remotely-sensed vegetation index data across a tropical forest restoration project area in Kibale National Park, Uganda, and evaluates the utility of vegetation indices to monitor the progress of forest regeneration.

This article has been accepted for publication and undergone full peer review but has not been through the copyediting, typesetting, pagination and proofreading process which may lead to differences between this version and the Version of Record. Please cite this article as doi: 10.1002/ldr.4096

Running title: Vegetation greening along a restoration gradient

Abstract

Restoration has now emerged as a global priority, with international initiatives such as the "UN Decade on Ecosystem Restoration (2021-2030)". To fulfil the large-scale global restoration ambitions, an essential step is the monitoring of vegetation recovery after restoration interventions. The aim of this study was to evaluate the utility of remotely-sensed vegetation indices, Normalized Difference Vegetation Index (NDVI) and Enhanced Vegetation Index (EVI), to monitor the progress of forest regeneration across a tropical forest restoration project area in Kibale National Park, Uganda. Using the chronosequence approach, results indicated non-linear patterns in NDVI and EVI across the first 25 years of recovery. Both NDVI and EVI increased for the first 10 years of forest regeneration. This "greening" phase could be used as the indicator of successful onset of forest recovery. In particular, the decline of elephant grass, and the consequent arrival of shrubs and trees, can be detected as an increase in NDVI. Primary forests differed from the 25-year-old regenerating forests based on the unique combination of low mean and low seasonal variation in EVI. Our results, therefore, suggest that the long-term success of forest restoration could be monitored by evaluating how closely the combination of mean, and degree of seasonal variation in EVI, resembles that observed in the primary forest.

Keywords: Africa – EVI – NDVI – restoration – tropical forest – vegetation index

Introduction

The rapid loss of tropical forests (Hansen et al., 2013; FAO, 2015) has profound consequences on biodiversity and ecosystem functioning (Chapin et al., 2000; Millennium Ecosystem Assessment, 2005). Even where the forest is allowed to recover, natural regeneration is not always sufficient to ensure forest recovery (Paul, Randle, Chapman, & Chapman, 2004). Natural regeneration can fail especially if large forest areas have already been lost, seed-sources are far away, or soils have lost their fertility (Arroyo-Rodríguez et al., 2017). Also, fast-colonizing pioneer vegetation (e.g., grasses or shrubs), together with fire, can arrest forest succession (Duclos, Boudreau, & Chapman, 2013; Wheeler et al., 2016). In such cases, active restoration measures (e.g., planting seedlings or spreading seeds), or passive restoration measures that remove human disturbances (e.g., excluding grazing or protection from fire) are needed to enable forest recovery (Lamb, Erskine, & Parrotta, 2005; Shono, Cadaweng, & Durst, 2007).

Restoration of forests has now emerged as a global priority, with international initiatives such as the "UN Decade on Ecosystem Restoration (2021-2030)" (UN, 2021) and "The Bonn Challenge" (IUCN, 2020). To fulfil the large-scale global restoration ambitions, an essential step is the monitoring of vegetation recovery after restoration interventions (Ruiz-Jaen & Aide, 2005). Typically, restoration success is monitored with field-measured attributes, e.g., vegetation cover, tree density or biomass, but frequent field assessments can be challenging with limited monitoring budgets (Ruiz-Jaen & Aide, 2005; Viani et al., 2017). The development of remote monitoring technologies could enable cost-effective assessment of vegetation recovery (Reif & Theel, 2017). For example, unmanned aerial vehicles can be used in monitoring tropical forest recovery (Zahawi et al., 2015; Reis et al., 2019). Other potential sources of data are satellite-based vegetation indices, Normalized Difference Vegetation Index (NDVI) and Enhanced Vegetation Index (EVI), which have been commonly used to measure vegetation activity at the land surface (Huete, Didan, van Leeuwen, Miura, & Glenn, 2011; Didan & Munoz, 2019).

Vegetation indices measure the "greenness" of the canopy, i.e., a combination of leaf chlorophyll content, leaf area, canopy cover and canopy structure (Glenn, Huete, Nagler, & Nelson, 2008; Didan & Munoz, 2019). These indices are based on the biological phenomenon that chlorophyll a and b in plant leaves absorb red wavelengths, while plant leaves scatter near-infrared (NIR) wavelengths (Tucker, 1979). Both NDVI and EVI are low in areas with sparse vegetation cover (deserts), intermediate in shrublands and savannas (with high seasonal variation in grassland ecosystems) and reach the highest values in broadleaved forests (Huete et al., 2011). In the tropics, vegetation indices have been previously used for land-cover classification and to detect land-cover dynamics (Tucker, Townshend, & Goff 1985; Hartter, Ryan, Southworth, & Chapman, 2011; Setiawan, Yoshino, & Prasetyo, 2014; Vijith & Dodge-Wan, 2020; Wanyama, Moore, & Dahlin, 2020), map forest disturbances (Murillo-Sandoval, Van Den Hoek, & Hilker, 2017), predict forest resilience to drought (Verbesselt et al., 2016), monitor natural succession (Caughlin et al., 2021), estimate large-scale patterns in biomass (Anaya, Chuvieco, & Palacios-Orueta, 2009) or primary production (Sjöström et al., 2011), and detect seasonal phenological rhythms and photosynthetic capacity (Xiao, Hagen, Zhang, Keller, & Moore, 2006; Brando et al., 2010; Valtonen et al., 2013). For example, in the Amazon, the first phase of forest regrowth can be detected as an increase in NDVI (Steininger, 1996). Outside tropics, vegetation indices have been used to monitor vegetation change across restoration and afforestation areas (Verbesselt, Hyndman, Newnham, & Culvenor, 2010; Sun et al., 2015; Zhang et al., 2016; Wu, Yu, Zhang, Du, & Zhang, 2019; Wang et al., 2020). However, to our knowledge, studies exploring the utility of remotely-sensed vegetation indices for monitoring the tropical forest recovery following restoration activities are yet lacking.

In this work, we assessed 20 years of vegetation index data across a tropical forest restoration project area in Kibale National Park, Uganda, together with field-based vegetation monitoring dataset. Our goal was to evaluate the utility of remotely-sensed vegetation indices to monitor the progress of forest regeneration in Afrotropics, where studies evaluating the restoration success have

been generally scarce (Ruiz-Jaen & Aide, 2005). The restoration project was established in 1994 in an area where elephant grass (*Cenchrus purpureus* (Schumach.) Morrone), a species native to eastern and central Africa, and fires, suppressed the natural regeneration of tree seedlings and thereby prevented forest recovery (UWA-FACE, 2015; Ssekuubwa et al., 2021). In this area, active restoration (i.e., planting with native trees and fire prevention), and passive restoration (i.e., fire prevention), has taken place since 1995. The restoration planting has produced an increase in tree stem density, above-ground biomass, and shrub cover, and decrease in grass cover (Wheeler et al., 2016). However, the cover of an invasive shrub *Lantana camara* has increased in the planted areas (Wheeler et al., 2016).

Our specific study questions were: 1) Does the vegetation greenness of restored forests converge to the level observed in the nearby primary forest (the target state of restoration), as the restored forests age? 2) How does the vegetation greenness in the restored forests, and in the primary forest, vary seasonally? 3) How do the remotely-sensed vegetation index values relate to ground-measured stand basal area, shrub cover or elephant grass cover?

We hypothesize that as the restored forests mature and age, leaf biomass, leaf area and canopy cover first increase, and then converge to levels observed in the nearby primary forest (Foody & Curran, 1994; Wheeler et al., 2016). We predict that these changes produce an increase in vegetation greenness, which should converge to levels observed in the primary forest. Alternatively, intermediate-aged regenerating forests, with a fast turnover of leaves in the canopy, could appear greener than the primary forest canopy, with older tree leaves hosting epiphyll growth, necroses and damage (Roberts, Nelson, Adams, & Palmer, 1998). In this case, vegetation greenness could be observed to reach its maximum in intermediate-aged regenerating forests.

2. Materials and Methods

2.1 Study area

This study was conducted in Kibale National Park (Figure 1), located within the Albertine Rift, Western Uganda (Struhsaker, 1997; Plumptre et al., 2003; Hartter et al., 2011). Kibale National Park (795 km^2, 900–1590 m a.s.l.) represents medium-altitude tropical moist forest but includes also reforestation areas, areas that have transitioned from forest to agriculture, grasslands and wetlands (Laporte, Walker, Stabach, & Landsberg, 2008; Hartter et al., 2011). The mean monthly temperature ranges between 20.8 and 22.1°C (Figure S1, Supplementary Material), and the study area has two distinct rainy seasons from March to May and from August to November, with a long-term mean annual precipitation of 1,475 mm (Struhsaker, 1997).

Kibale National Park hosts over 500 plant species, of which 330 are trees (Plumptre et al., 2003). In the mature forest, trees reach over 30 m height, the forest has a closed overstory canopy, with little or no herbaceous vegetation in the understory, or light reaching the understory (Wing & Buss, 1970). Seven secondary successional vegetation types have been described in Kibale; tall grass, followed by Acanthus-grass, Acanthus-grass-scrub, colonizing forest, and three distinct forest types with decreasing cover of herbaceous vegetation in the understory, and gradual development of overstory and understory canopy layers (Wing & Buss, 1970). Common species in the early stages are elephant grass and *Hyparrhenia* spp. grasses and *Acanthus pubescens* Engl. shrub. Arrested succession is common in Kibale, where the aforementioned grasses and shrubs, together with invasive shrub *Lantana camara* L. and fire, can prevent forest regeneration (Paul et al., 2004; Lawes & Chapman, 2006; Duclos et al., 2013; Wheeler et al., 2016).

2.2 Restoration project area

Kibale National park has an approximately 10,000 ha restoration project area run by the Uganda Wildlife Authority (UWA) and Forests Absorbing Carbon dioxide Emission (FACE) the future

foundation (Omeja et al., 2011; UWA-FACE, 2015; Wheeler et al., 2016) (Figure 1; Figure S2, Supplementary Material). In this part of the park, elevation ranges between 1,000 and 1,440 m a.s.l. (IRI/LDEO Climate Data Library, 2020). The project was established to an area where moist semi-deciduous forests were largely cut down by agricultural encroachers in the 1970s and 1980s (Struhsaker, 1997; Chapman & Lambert, 2000; UWA-FACE, 2015). After settlers were relocated, the area was largely colonized by elephant grass, and together with fire, it suppressed naturally regenerating tree seedlings and thereby prevented forest recovery (UWA-FACE, 2015; Wheeler et al., 2016). Active restoration planting, along with protection from fire, has taken place annually since 1995 (UWA-FACE, 2015) (the exceptions being years 2001 and 2013-2015, when no planting took place; see details in Figures S2-S3, Supplementary Material). The native trees planted (400 ha^{-1}) included *Bridelia micrantha* (Hochst.) Baill, *Cordia africana* Lam, *Cordia ugandensis* S.Moore, *Croton macrostachys* Hochst. ex A.Rich., *Croton megalocarpus* Hutch, *Ficus natalensis* Hochst, *Mimusops bagshawei* S.Moore, *Prunus africana* (Hook.f.) Kalkman, *Spathodea campanulata* P.Beauv., and *Warburgia ugandensis* Sprague (Omeja et al., 2011; UWA-FACE, 2015; Wheeler et al., 2016). Field assessments in 2005 and 2013 have shown that the restoration planting has been generally successful, with increasing trends in tree stem density and above-ground biomass (Wheeler et al., 2016).

The restoration project area also includes large areas representing passive restoration (Ssekuubwa et al., 2021), i.e., protection of natural regrowth from fire (Figure 1). These are areas where the forest was cleared in the past, but natural regeneration was feasible (Ssekuubwa et al., 2021). To the east, the restoration project area is bordered by a belt of primary forest (Figure 1), herein referred to as the reference area, i.e., the target state of the restoration.

2.3 Vegetation indices

The two most commonly used vegetation indices, NDVI and EVI, were included in this work. The values of NDVI range between -1 and +1 so that areas with higher canopy greenness receive the highest positive values (Glenn et al., 2008; Didan & Munoz, 2019). The values of NDVI are calculated as follow:

$$NDVI = \frac{NIR - Red}{NIR + Red}$$

where *NIR* and *Red* indicate the reflectance values of NIR and red light, respectively. Across Africa, NDVI is low in areas with sparse vegetation cover (e.g., Sahara and Sahelian zone) and reaches the highest values in dense humid forests (Tucker et al., 1985; Goetz & Prince, 1999). However, NDVI tends to saturate when vegetation density is very high (Huete et al., 2002). EVI was developed to perform better in high biomass regions, for improved de-coupling of canopy-background signal, as well as to reduce atmospheric influences (Huete et al., 2002; Didan & Munoz, 2019). The values of EVI are calculated as follow (Didan & Munoz, 2019):

$$EVI = 2.5 \times \frac{NIR - Red}{NIR + 6 \times Red - 7.5 \times Blue + 1}$$

where *Blue* indicates the reflectance value of blue light. We included both NDVI and EVI because they could complement each other. NDVI has a higher dynamic range in low greenness values, and therefore better ability to separate semiarid habitat types from each other, while EVI has a higher dynamic range in high greenness values, and is better in separating humid forested habitat types from each other (Huete et al., 2002).

We used the Terra Moderate Resolution Imaging Spectroradiometer (MODIS) Vegetation Indices (MOD13Q1) Version 6 dataset (Didan & Munoz, 2019; USGS, 2020). This data represents 16-day NDVI and EVI composites at 250 × 250 m spatial resolution. The composites are generated with an algorithm that chooses the best available pixel value from the 16-day period. The NDVI and EVI datasets were downloaded from IRI/LDEO Climate Data Library (2021a), and the vegetation

index quality data from IRI/LDEO Climate Data Library (2021b). We determined the validity of vegetation index values following the four criteria used in Samanta et al. (2010) and Samanta, Ganguly, Vermote, Nemani, and Myneni (2012a). The vegetation index value was considered valid and selected for further analyses, if: 1) "VI Quality" was "good quality" or "check other quality assessment (QA)". 2) "VI Usefulness", which has 16 levels (Didan & Munoz, 2019) ranged between 0 and 11. 3) Clouds were absent, i.e., no "adjacent cloud detected", no "mixed clouds", and no "possible shadow". 4) "Aerosol quantity" was either "low" or "intermediate".

The NDVI and EVI datasets were downloaded across a rectangular area 30.26 – 30.41°E, and 0.25 – 0.50°N covering a total of 7,866 grids (at 250 × 250 m spatial resolution), including both the restoration area and nearby primary forests. For each grid, the NDVI and EVI values were available, and downloaded, between 30 April 2000 and 25 December 2020. This time span covers a total of 476 potential time-points (the 16-day composites), and each fully covered year has 23 time-points. These search criteria produced a total of 3,724,858 vegetation index values for each NDVI and EVI. Based on vegetation index quality data, 2,790,260 (75%) of these values were considered valid and were selected for further analyses.

2.4 Grid selection and management classes

Out of the 7,866 grids, a total of 2,853 grids were selected for further analyses (Figure 1; Figure S3, Supplementary Material). The grid was selected if its center was located either inside the planted areas or inside areas designated for passive restoration, or if it represented primary forest. Primary forest grids (Figure 1) excluded grids classified as "degraded forest" in earlier land-classifications (UWA-FACE, 2015).

We further classified the 2,853 grids to seven management classes: 1) Primary forest (1,719 grids), 2) Passive restoration (430 grids), 3) Planted 1995–1999 (396 grids), 4) Planted 2000–2004

(76 grids), 5) Planted 2005–2009 (106 grids), 6) Planted 2010–2011 (81 grids), and 7) Planted 2016–2020 (45 grids). This classification aimed to divide the planting years into 5-year intervals. However, since no planting took place between 2013 and 2015, and the 2012 planted area was so small that it contained no grids (Figure S3, Supplementary Material), one management class (Planted 2010–2011) includes only two planting years.

2.5 Vegetation measurements

To study how NDVI and EVI are related to the field-measured characteristics of the vegetation, we extracted data across 174 vegetation monitoring study sites (Figure S2, Supplementary Material), censused in 2013 (Owiny et al., unpublished). At each study site, large trees (> 20 cm diameter at breast height; DBH) were censused in a 40 m × 20 m plot. Small trees and poles (10–20 cm DBH) were censused in a 20 m × 20 m plot, saplings (5–10 cm DBH) in a 20 m × 10 m plot, and seedlings (< 5 cm DBH) in a 10 m × 10 m plot; all plots being nested and sharing one corner. For each study site, we estimated the stand basal area (m^2 ha^{-1}) based on trees with DBH ≥ 5 cm. The basal area has been frequently used as a surrogate of forest biomass (Brown, Gillespie, & Lugo, 1989). We also used the visually estimated shrub and elephant grass covers for each 40 × 20 m plot. The cover values were estimated on a scale: 0 (0%), 0.5 (<10%), 1 (10%), 2 (20%), 3 (30%),…, 10 (100%).

2.6 Statistical analyses

We first used chronosequence approach to find out if the vegetation greenness of the restored forests converges through time to levels observed in the nearby primary forest. The mean NDVI and EVI in 2020 was calculated for each grid representing active or passive restoration (1,134 grids). The year 2020 was selected to maximize the length of the chronosequence. For each grid, we calculated the forest age (years since restoration started). Grids representing passive restoration

were assigned forest age 25 years. For each forest age, mean vegetation greenness (across grids) was plotted along the chronosequence.

To model the pattern in vegetation greenness along the chronosequence, three competing models were fitted, with mean NDVI or EVI for each forest age as the response and forest age as the predictor variable: 1) linear model, 2) three-parameter asymptotic exponential model, which allows the greenness to slowly approach an asymptote, fitted with self-starting non-linear function "SSasymp" in R (R Core Team, 2021), and 3) quadratic model allowing greenness to first increase and then decrease. The fit of the three competing models was compared with the second-order Akaike Information Criterion (AICc; Burnham & Anderson, 2002) calculated with package "MuMIn" in R (R Core Team, 2021).

For each of the seven management classes, we calculated mean annual and mean monthly NDVI and EVI. These were calculated from the full time-series with 476 time-points (the 16-day composites) representing mean NDVI and EVI values for each of the seven management classes (mean across the grids). These time-series included some missing values (4–14%), due to missing time-points in the original MODIS datasets, and due to omission of poor-quality data (based on the vegetation index quality data, see above). The missing values in the seven time-series were replaced with linear interpolation using package "imputeTS" in R (R Core Team, 2021).

To illustrate the 20-year time-trends in the vegetation greenness of each management class, the mean annual NDVI and EVI were plotted between 2001-2020 (excluding 2000 which was not fully covered). Time trends were modelled with Generalized Additive Models (GAMs), using package "mgcv" in R (R Core Team, 2021), and following Zuur, Ieno, Walker, Saveliev, and Smith (2009, p. 43), with cross-validation used to estimate the optimal amount of smoothing for the smoothing term (the explanatory variable) and with cubic regression splines. We further pooled the data of all management classes and modelled the mean annual greenness as a function of year (representing the time-trend), management class, and their interaction, by fitting a Generalized least

squares model with auto-regressive model of order one (AR-1) structure for the year, following Zuur et al. (2009, p. 149). The AR-1 structure takes into account the possible temporal autocorrelation in the residuals, i.e., the closer two time-points are in time, the higher the correlation.

To describe the seasonal patterns in vegetation greenness, the mean monthly NDVI and EVI of each management class, was first plotted together with mean monthly precipitation (see sources in Figure S4, Supplementary Material). Cross-correlations between monthly time-series (N = 249) of greenness and precipitation were calculated with function "ccf" in R (R Core Team, 2021). We also illustrated how the degree of seasonal variation in NDVI or EVI relates to their mean values (Requena-Mullor, Reyes, Escribano, & Cabello, 2018) across the seven management classes. As a measure of the degree of seasonal variation, we used coefficient of variation (CV) calculated from the mean monthly values.

Finally, we described how NDVI and EVI are related to the three field-measured structural characteristics of the vegetation (stand basal area, shrub cover, elephant grass cover). The 174 vegetation study sites were located in 146 grids (250 × 250 m) from which data of NDVI and EVI was available. For each of these 146 grids, we calculated the mean value for each of the three vegetation structure variables, and the mean of NDVI and EVI in 2013, i.e., the year of the vegetation census. To describe associations between NDVI or EVI (the response) and each of the three vegetation structure variables (the predictors), GAMs were fitted following the same method as detailed above. All statistical analyses were run with R version 4.0.3 (R Core Team, 2021).

3. Results

3.1 Do NDVI and EVI converge through time to level of primary forest?

The patterns of both NDVI and EVI along the chronosequence were best described with the quadratic models (Figure 2; Table S1, Supplementary Material). Both NDVI and EVI increased for the first 10 years of forest regeneration but after 20 years, both start to decline towards lower levels observed in the primary forest.

The pattern of vegetation greening after restoration planting is also visible in the annual time-series of NDVI and EVI (Figures S5-S6, Supplementary Material). Based on the Generalized least squares model, there was a significant overall long-term trend in mean annual NDVI ($F_{1, 126} = 76.9$, $p < 0.001$), overall differences among management classes ($F_{6, 126} = 130.2$, $p < 0.001$), but the slopes of the long-term trends differed among management classes (year × management class interaction; $F_{6, 126} = 5.2$, $p < 0.001$). There was also a significant overall long-term trend in mean annual EVI ($F_{1, 126} = 24.8$, $p < 0.001$), overall differences among management classes ($F_{6, 126} = 29.0$, $p < 0.001$), but the year × management class interaction was not significant ($F_{6, 126} = 2.1$, $p = 0.060$).

3.2 Seasonal pattern in NDVI and EVI

Both NDVI and EVI follow clear seasonal patterns; the two annual greenness peaks follow precipitation peaks with approximately one-month time-lag (Figure 3; Figures S7-S8, Supplementary Material). The seasonal variation is generally larger, and greenness peaks narrower, in the management class Planted 2016-2020, which represents mostly elephant grass during our study period. The seasonal variation in greenness (measured as CV) generally decreases as the mean level of greenness increases (Figure S9, Supplementary Material). The primary forest can be distinguished from regenerating forests by the unique combination of low seasonal variation and low mean level in EVI. On the contrary, a combination of CV and mean level in NDVI cannot be used to distinguish the primary forest from regenerating forests.

3.3 How vegetation indices relate to ground-measured vegetation structure?

NDVI peaks when stand basal area reaches approx. 10 m^2 ha^{-1}, and declines in values higher than this (GAM; estimated degrees of freedom (edf) = 4.7, F = 15.6, $p < 0.001$; Figure 4A). Also, EVI peaks when stand basal area reaches approx. 10 m^2 ha^{-1}, but declines steeply in values higher than this (GAM; edf = 5.0, F = 19.8, $p < 0.001$; Figure 4B).

Furthermore, both NDVI (edf = 1.0, F = 6.25, p = 0.014; Figure 4C), and EVI increase as shrub cover increases (edf = 2.5, F = 24.4, $p < 0.001$; Figure 4D). On contrary, NDVI decreases steeply as the elephant grass cover increases (edf = 2.8, F = 45.0, $p < 0.001$; Figure 4E) while association between EVI and elephant grass cover is non-significant (edf = 2.1, F = 1.6, p = 0.199; Figure 4F).

4. Discussion

Our results show that the onset of tropical forest regeneration, after restoration interventions, can be detected as an increase in vegetation greenness. This "greening" phase, detected both in the chronosequence (Figure 2), and in the annual time-series (Figures S5-S6, Supplementary Material), takes place when the tree basal area increases up to 10 m^2 ha^{-1} (Figure 4). The common shrub species, *Acanthus pubescens* and *Lantana camara*, are likely to contribute significantly to the observed greening pattern (Figure 4; Wheeler et al., 2016). Notably, the decline of the elephant grass, and the consequent arrival of shrubs and trees (Wheeler et al., 2016), is detectable as an increase in NDVI (Figure 4). The duration of this greening phase is likely to depend on environmental conditions, and severity of disturbance and could differ among geographical regions. For example, in the Amazon, NDVI increased to levels similar to the primary forest in only a few years of regeneration (Steininger, 1996).

Vegetation greenness reached its maximum in intermediate-aged regenerating forests (Figure 2), indicating that neither NDVI nor EVI can be used as simple measures of long-term forest recovery. In our study area, the intermediate-aged regenerating forests are characterized by dense thickets of shrubs, mainly composed of *Acanthus pubescens* and other large-leaved shrubs and herbs, such as *Triumfetta* sp., *Aframomum* sp., *Lantana camara* and *Marantochloa leucantha* (K.Schum.) Milne-Redh. (pers. obs.). When the canopy cover reaches 100%, vegetation indices measure the greenness of the plant species forming the canopy, and plant species can differ markedly in their canopy greenness (Glenn et al., 2008). The canopy of the intermediate-aged forests can appear greener than the canopy of primary forest if the canopy is dominated by plant species which have particularly high chlorophyll content or canopy architecture producing high greenness (Glenn et al., 2008), or if there is a faster turnover in canopy leaves. Early successional fast-growing trees, shrubs and forbs tend to have lower leaf longevity than slower-growing late-successional trees (King, 1994; Kikuzawa & Ackerly, 1999; Ishida et al., 2008). As the tree leaves age, they accumulate epiphyll growth, necroses and damages, which are detectable as changes in NIR (Roberts et al., 1998). Moreover, EVI is more sensitive to changes in NIR than NDVI (Huete, et al., 2011). This could explain why after 20 years of recovery, EVI (and less so NDVI) started to decline towards levels observed in the primary forest. Presumably, in this "browning" phase, late-successional tree canopies increasingly cover shrubs of the understory. Further studies are needed to find out if, and when, the greenness of the restored forests finally converge to the primary forest level.

Our results largely comply with previous observations across the tropics. Higher levels of NDVI in regenerating forests, compared to primary forests, was previously reported in Kibale NP by Hartter et al. (2011). In the Amazon, regenerating tropical forests, between 5 to 20 years old, showed NDVI comparable, or slightly higher, than the primary forest (Steininger, 1996). In Borneo, the rapid regrowth of secondary vegetation after logging (classified as woody savannas and

grasslands) showed slightly higher EVI than the evergreen broad-leaved forests, i.e., vegetation prior to logging, but overall, these vegetation types were not distinguishable based on EVI (Vijith & Dodge-Wan, 2020). The levels of NDVI and EVI in our data comply with previous observations from a seasonal tropical humid broad-leaved forest in Tapajos, Brazil (Huete et al., 2002) and tropical broad-leaved forest in Borneo (Vijith & Dodge-Wan, 2020); both of these works were based on MODIS datasets as used in this work. However, the level of NDVI in our data was higher than what was previously reported in Kibale NP by Hartter et al. (2011) but slightly lower than reported in the Amazon (Steininger, 1996); both works based on Landsat images. As noted by Huete et al. (2002), vegetation index values produced by different sensors can deviate especially across high greenness values.

The biomass of tropical forests cannot be simply predicted based on satellite-derived NDVI or EVI, because the associations are strongly non-linear (Figure 4). Also, several previous works have failed to establish correlations between tropical forest biomass and NDVI (Foody et al., 2001; Foody, Boyd, & Cutler, 2003; Freitas, Mello, & Cruz, 2005) or EVI (Anaya et al., 2009). We assume that the peak of greenness at stand basal area 10 m^2 ha^{-1} is explained by the dense shrub cover in this regeneration phase. Our results imply that "browning" trends (de Jong, Verbesselt, Zeileis, & Schaepman, 2013; Higginbottom & Symeonakis, 2020), are not necessarily only a sign of human disturbance (Murillo-Sandoval et al., 2017), or drought (Anyamba & Tucker, 2005), but in some cases could also be a sign of increasing forest biomass and ecosystem recovery. Furthermore, all "greening" trends may not be indicative of an increase in biomass. For example, in Senegal, the transition from woody vegetation to the dominance of shrubs was detected as increased NDVI (Herrmann & Tappan, 2013).

The long-term success of forest restoration could be monitored by evaluating how closely the combination of mean, and degree of seasonal variation in EVI, resembles that observed in the primary forest, i.e., the target state of restoration. NDVI is not suitable for this purpose, presumably

because it saturates as the vegetation density becomes very high (Huete et al., 2002; Didan & Munoz, 2019). Previously, the combination of mean and seasonal variation of vegetation greenness has been used to classify vegetation types on landscape or continental level (Paruelo, Jobbagy, & Sala, 2001; Alcaraz-Segura, Paruelo, Epstein, & Cabello, 2013; Requena-Mullor et al., 2018). As shown by our study (Figure 3), and previous studies (e.g., Brando et al., 2010), NDVI and EVI are highly useful for understanding the seasonal patterns in tropical rain forests. The bi-annual seasonal pattern in vegetation greenness can be mechanistically explained by the leaf flush during and after the rainy season (Brando et al., 2010; Samanta et al., 2012b). During dry-season, vegetation greenness decreases as leaves dry, or age and accumulate epiphyll growth, leaf necrosis and damage (Roberts et al., 1998; Samanta et al., 2012b). The generally smaller seasonal variation in greenness in forests, compared to grasslands, is likely explained by the ability of trees to buffer drought with their deep roots (Anderson et al., 2015), although it is also known that large trees could be more susceptible to droughts than smaller trees (Bennett, McDowell, Allen, & Anderson-Teixeira, 2015). However, as the forest structure becomes more complex during succession, the multiple leaf and canopy layers are likely to produce smaller seasonal variations in canopy greenness compared to structurally less complex younger forests.

To conclude, remotely-sensed vegetation indices can provide valuable information to monitor forest recovery after restoration interventions. NDVI and EVI datasets can be used as cost-effective tools in monitoring vegetation recovery across large-scale restoration or afforestation areas. Grids where the "greening" phase is not detected could be inspected in the field, enabling corrective actions to take place. For monitoring the transition from grassland to tropical forest, NDVI and EVI complement each other. NDVI is more sensitive in detecting the withdrawal of the grasses, while EVI could be more sensitive for detecting the different successional stages between intermediate-aged regenerating and primary forest. As a result, the "greening phase" of the first 10 years of forest regeneration could be used as the indicator of successful onset of forest recovery, while the long-

term success of forest restoration could be monitored by evaluating how closely the combination of mean, and degree of seasonal variation in EVI, resembles that observed in the primary forest. Previous works in the restoration area of Kibale NP, Uganda, have reported the successful establishment of the planted trees, natural regeneration of several tree species (Omeja et al., 2011), and recovery-patterns in tree communities (Wheeler et al., 2016), fruit-feeding butterfly communities (Nyafwono, Valtonen, Nyeko, & Roininen, 2014) and bird communities (Latja, Valtonen, Malinga, & Roininen, 2016). In the future, remote sensing could be also utilized to predict recovery of diversity patterns (Khare, Latifi, & Rossi, 2019; Laliberte, Schweiger, & Legendre, 2020) or to monitor invasive species (Royimani, Mutanga, Odindi, Dube, & Matongera, 2019), such as the invasive shrub *Lantana camara*, across large-scale restoration areas.

Acknowledgements

We thank M. Matikainen and L. Leinonen for help with downloading the MODIS datasets, A. Owiny for vegetation data, W. van Goor and A. Hiltunen for help with the maps, and the Academy of Finland for funding (Project 324392 to A.V.).

References

Alcaraz-Segura, D., Paruelo, J. M., Epstein, H. E., & Cabello, J. (2013). Environmental and human controls of ecosystem functional diversity in temperate South America. *Remote Sensing, 5,* 127–154. doi:10.3390/rs5010127

Anaya, J. A., Chuvieco, E., & Palacios-Orueta, A. (2009). Aboveground biomass assessment in Colombia: A remote sensing approach. *Forest Ecology and Management, 257*, 1237–1246. doi:10.1016/j.foreco.2008.11.016

Anderson, M. C., Zolin, C. A., Hain, C. R., Semmens, K., Yilmaz, M. T., & Gao, F. (2015). Comparison of satellite-derived LAI and precipitation anomalies over Brazil with a thermal infrared-based Evaporative Stress Index for 2003-2013. *Journal of Hydrology 526,* 287–302. doi:10.1016/j.jhydrol.2015.01.005

Anyamba, A., & Tucker, C. J. (2005). Analysis of Sahelian vegetation dynamics using NOAA-AVHRR NDVI data from 1981–2003. *Journal of Arid Environments, 63*, 596–614. doi:10.1016/j.jaridenv.2005.03.007

Arroyo-Rodríguez, V., Melo, F. P. L., Martínez-Ramos, M., Bongers, F., Chazdon, R. L., Meave, J. A., … Tabarelli, M. (2017). Multiple successional pathways in human-modified tropical landscapes: new insights from forest succession, forest fragmentation and landscape ecology research. *Biological Reviews, 92*, 326–340. doi:10.1111/brv.12231

Bennett, A. C., McDowell, N. G., Allen, C. D., & Anderson-Teixeira, K. J. (2015). Larger trees suffer most during drought in forests worldwide. *Nature Plants, 1,* 15139. doi: 10.1038/NPLANTS.2015.139

Brando, P. M., Goetz, S. J., Baccini, A., Nepstad, D. C., Beck, P. S. A., & Christman, M. C. (2010). Seasonal and interannual variability of climate and vegetation indices across the Amazon. *Proceedings of the National Academy of Sciences of the United States of America, 107*, 14685–14690. doi:10.1073/pnas.0908741107

Brown, S., Gillespie, A. J. R., & Lugo, A. E. (1989). Biomass estimation methods for tropical forests with applications to forest inventory data. *Forest Science, 35*, 881–902. doi:10.1093/forestscience/35.4.881

Burnham, K. P., & Anderson, D. R. (2002). *Model selection and multi-model inference: a practical information-theoretic approach.* Secausus, NJ: Springer.

Caughlin, T. T., Barber, C., Asner, G. P., Glenn, N. F., Bohlman, S. A., & Wilson, C. H. (2021). Monitoring tropical forest succession at landscape scales despite uncertainty in Landsat time series. *Ecological Applications, 31*, Article e02208. doi:10.1002/eap.2208

Chapin, F. S., Zavaleta, E. S., Etviner, V. T., Naylor, R. L., Vitousek, P. M., Reynolds, H. L., … Díaz, S. (2000). Consequences of changing biodiversity. *Nature, 405*, 234–242. doi:10.1038/35012241

Chapman, C. A., & Lambert, J. E. (2000). Habitat alteration and the conservation of African primates: case study of Kibale National Park, Uganda. *American Journal of Primatology, 50,* 169–185. doi:10.1002/(SICI)1098-2345(200003)50:3<169::AID-AJP1>3.0.CO;2-P

de Jong, R., Verbesselt, J., Zeileis, A., & Schaepman M. E. (2013). Shifts in global vegetation activity trends. *Remote Sensing, 5,* 1117–1133. doi:10.3390/rs5031117

Didan, K., & Munoz, A. B. (2019). *MODIS Vegetation index user's guide. (MOD13 Series). Version 3.1, September 2019.* Retrieved from https://vip.arizona.edu/documents/MODIS/MODIS_VI_UsersGuide_09_18_2019_C61.pdf

Duclos, V., Boudreau, S., & Chapman, C. A. (2013). Shrub cover influence on seedling growth and survival following logging of a tropical forest. *Biotropica*, *45*, 419–426. doi:10.1111/btp.12039

FAO. (2015). *Global Forest Resources Assessment 2015. How are the world's forests changing?* Rome: FAO.

Foody, G. M., Boyd, D. S., & Cutler, M. E. J. (2003). Predictive relations of tropical forest biomass from Landsat TM data and their transferability between regions. *Remote Sensing of Environment, 83*, 463–474. doi:10.1016/S0034-4257(03)00039-7

Foody, G. M., & Curran, P. J. (1994). Estimation of tropical forest extent and regenerative stage using remotely sensed data. *Journal of Biogeography, 21*, 223–244. doi:10.2307/2845527

Foody, G. M., Cutler, M. E., McMorrow, J., Pelz, D., Tangki, F., Boyd, D. S., & Douglas, I. (2001). Mapping the biomass of Bornean tropical rain forest from remotely sensed data. *Global Ecology & Biogeography, 10*, 379–387. doi:10.1046/j.1466-822X.2001.00248.x

Freitas, S. R., Mello, M. C. S., & Cruz, C. B. M. (2005). Relationships between forest structure and vegetation indices in Atlantic Rainforest. *Forest Ecology and Management, 218*, 353–362. doi:10.1016/j.foreco.2005.08.036

Glenn, E. P., Huete, A. R., Nagler, P. L., & Nelson, S. G. (2008). Relationship between remotely-sensed vegetation indices, canopy attributes and plant physiological processes: what vegetation indices can and cannot tell us about the landscape. *Sensors, 8*, 2136–2160. doi:10.3390/s8042136

Goetz, S. J., & Prince, S. D. (1999). Modelling terrestrial carbon exchange and storage: evidence and implications of functional convergence in light-use efficiency. *Advances in Ecological Research, 28*, 57–92. doi:10.1016/S0065-2504(08)60029-X

Hansen, M. C., Potapov, P. V., Moore, R., Hancher, M., Turubanova, S. A., Tyukavina, A., … Townshend, J. R. G. (2013). High-resolution global maps of 21st-century forest cover change. *Science, 342*, 850–853. doi:10.1126/science.1244693

Hartter, J., Ryan, S. J., Southworth, J., & Chapman, C. A. (2011). Landscapes as continuous entities: forest disturbance and recovery in the Albertine Rift landscape. *Landscape Ecology, 26*, 877–890. doi:10.1007/s10980-011-9616-0

Herrmann, S. M., & Tappan, G. G. (2013). Vegetation impoverishment despite greening: a case study from central Senegal. *Journal of Arid Environments, 90,* 55–66. doi: 10.1016/j.jaridenv.2012.10.020

Higginbottom, T. P., & Symeonakis, E. (2020). Identifying ecosystem function shifts in Africa using breakpoint analysis of long-term NDVI and RUE data. *Remote Sensing, 12,* Article 1894. doi: 10.3390/rs12111894

Huete, A., Didan, K., Miura, T., Rodriguez, E. P., Gao, X., & Ferreira, L. G. (2002). Overview of the radiometric and biophysical performance of the MODIS vegetation indices. *Remote Sensing of Environment, 83*, 195–213. doi:10.1016/S0034-4257(02)00096-2

Huete, A., Didan, K., van Leeuwen, W., Miura, T., & Glenn, E. (2011). MODIS Vegetation Indices. In B. Ramachandran, C. O. Justice, & M. J. Abrams (Eds.), *Land remote sensing and global environmental change. NASA's Earth Observing System and the Science of ASTER and MODIS* (pp. 579–602). New York: Springer.

IRI/LDEO Climate Data Library. (2020). *Select a Point Climatology. Elevation* [Dataset]. Retrieved from http://iridl.ldeo.columbia.edu/maproom/Global/Climatologies/Select_a_Point.html?maptype=elev

IRI/LDEO Climate Data Library. (2021a). *MODIS Analysis Tool* [Dataset]. Retrieved from http://iridl.ldeo.columbia.edu/maproom/Food_Security/Locusts/Regional/MODIS/index.html

IRI/LDEO Climate Data Library. (2021b). *USGS LandDAAC MODIS version_006 EAF VI_Quality* [Dataset]. Retrieved from http://iridl.ldeo.columbia.edu/SOURCES/.USGS/.LandDAAC/.MODIS/.version_006/.EAF/.VI_Quality/

Ishida, A., Nakano, T., Yazaki, K., Matsuki, S., Koike, N., Lauenstein, D. L., Shimizu, M., & Yamashita, N. (2008). Coordination between leaf and stem traits related to leaf carbon gain and hydraulics across 32 drought-tolerant Angiosperms. *Oecologia, 156*, 193–202. doi:10.1007/s00442-008-0965-6

IUCN. (2020). The Bonn Challenge. Retrieved from www.bonnchallenge.org/

Khare, S., Latifi, H., & Rossi, S. (2019). Forest beta-diversity analysis by remote sensing: how scale and sensors affect the Rao's Q index. *Ecological Indicators, 106,* Article 105520. doi: 10.1016/j.ecolind.2019.105520

Kikuzawa, K., & Ackerly, D. (1999). Significance of leaf longevity in plants. *Plant Species Biology, 14*, 39–45. doi:10.1046/j.1442-1984.1999.00005.x

King, D. A. (1994). Influence of light level on the growth and morphology of saplings in a Panamanian forest. *American Journal of Botany, 81*, 948–957. doi:10.2307/2445287

Laliberte, E., Schweiger, A. K., & Legendre, P. (2020). Partitioning plant spectral diversity into alpha and beta components. *Ecology Letters, 23,* 370–380. doi:10.1111/ele.13429

Lamb, D., Erskine, P. D., & Parrotta, J. A. (2005). Restoration of degraded tropical forest landscapes. *Science, 310*, 1628–1632. doi:10.1126/science.1111773

Laporte, N., Walker, W., Stabach, J., & Landsberg, F. (2008). Monitoring forest-savanna dynamics in Kibale National Park with satellite imagery (1989-2003): implications for the management of wildlife habitat. In R. Wrangham, & E. Ross (Eds.), *Science and conservation in African forests: the benefits of long-term research* (pp. 38–50). Cambridge: Cambridge University Press.

Latja, P., Valtonen, A., Malinga, G. M., & Roininen, H. (2016). Active restoration facilitates bird community recovery in an Afrotropical rainforest. *Biological Conservation, 200,* 70–79. doi: 10.1016/j.biocon.2016.05.035

Lawes, M. J. & Chapman, C. A. (2006). Does the herb *Acanthus pubescens* and/or elephants suppress tree regeneration in disturbed Afrotropical forest? *Forest Ecology and Management, 221*, 278–284. doi:10.1016/j.foreco.2005.10.039

Millennium Ecosystem Assessment. (2005). *Ecosystems and Human Well-being: Synthesis*. Washington, DC: Island Press.

Murillo-Sandoval, P. J., Van Den Hoek, J., & Hilker, T. (2017). Leveraging multi-sensor time-series datasets to map short- and long-term tropical forest disturbances in the Colombian Andes. *Remote Sensing, 9*, Article 179. doi:10.3390/rs9020179

Nyafwono, M., Valtonen, A., Nyeko, P., & Roininen, H. (2014). Fruit-feeding butterfly communities as indicators of forest restoration in an Afro-tropical rainforest. *Biological Conservation, 174,* 75–83. doi:10.1016/j.biocon.2014.03.022

Omeja, P. A., Chapman, C. A., Obua, J., Lwanga, J. S., Jacob, A. L., Wanyama, F., & Mugenyi, R. (2011). Intensive tree planting facilitates tropical forest biodiversity and biomass accumulation in Kibale National Park, Uganda. *Forest Ecology and Management, 261*, 703–709. doi:10.1016/j.foreco.2010.11.029

Paruelo, J. M., Jobbagy, E. G., & Sala, O. E. (2001). Current distribution of ecosystem functional types in temperate South America. *Ecosystems, 4,* 683–698. doi:10.1007/s10021-001-0037-9

Paul, J. R., Randle, A. M., Chapman, C. A., & Chapman, L. J. (2004). Arrested succession in logging gaps: is tree seedling growth and survival limiting? *African Journal of Ecology, 42*, 245–251. doi:10.1111/j.1365-2028.2004.00435.x

Plumptre, A. J., Behangana, M., Ndomba, E., Davenport, T., Kahindo, C., Kityo, R., … Owiunji, I. (2003). *The biodiversity of the Albertine Rift. Albertine Rift Technical Reports* (No. 3). Retrieved from https://portals.iucn.org/library/node/26890

R Core Team. (2021). R: A language and environment for statistical computing. R Foundation for Statistical Computing, Vienna, Austria. Retrieved from https://www.r-project.org/

Reif, M. K., & Theel, H. J. (2017). Remote sensing for restoration ecology: Application for restoring degraded, damaged, transformed, or destroyed ecosystems. *Integrated Environmental Assessment and Management, 13,* 614–630. doi:10.1002/ieam.1847

Reis, B. P., Martins, S. V., Filho, E. I. F, Sarcinelli, T. S., Gleriani, J. M., Leite, H. G., & Halassy, M. (2019). Forest restoration monitoring through digital processing of high resolution images. *Ecological Engineering, 127*, 178–186. doi:10.1016/j.ecoleng.2018.11.022

Requena-Mullor, J. M., Reyes, A., Escribano, P., & Gabello, J. (2018). Assessment of ecosystem functioning from space: Advancements in the Habitats Directive implementation. *Ecological Indicators, 89*, 893–902. doi:10.1016/j.ecolind.2017.12.036

Roberts, D. A., Nelson, B. W., Adams, J. B., & Palmer, F. (1998). Spectral changes with leaf aging in Amazon caatinga. *Trees, 12*, 315–325. doi:10.1007/s004680050157

Royimani, L., Mutanga, O., Odindi, J., Dube, T., & Matongera, T. N. (2019). Advancements in satellite remote sensing for mapping and monitoring of alien invasive plant species (AIPs). *Physics and Chemistry of the Earth, 112,* 237–245. doi:10.1016/j.pce.2018.12.004

Ruiz-Jaen, M. C., & Aide, T. M. (2005). Restoration success: how is it being measured? *Restoration Ecology, 13,* 569–577. doi:10.1111/j.1526-100X.2005.00072.x

Samanta, A., Ganguly, S., Hashimoto, H., Devadiga, S., Vermote, E., Knyazikhin, Y., Nemani, R. R., & Myneni, R. B. (2010). Amazon forests did not green-up during the 2005 drought. *Geophysical Research Letters, 37*, Article L054001. doi:10.1029/2009GL02154

Samanta, A., Ganguly, S., Vermote, E., Nemani, R. R., & Myneni, R. B. (2012a). Interpretation of variations in MODIS-measured greenness levels of Amazon forests during 2000 to 2009. *Environmental Research Letters, 7*, Article 024018. doi:10.1088/1748-9326/7/2/024018

Samanta, A., Knyazikhin, Y., Xu, L., Dickinson, R. E., Fu, R., Costa, M. H., … Myneni, R. B. (2012b). Seasonal changes in leaf area of Amazon forests from leaf flushing and abscission. *Journal of Geophysical Research, 17,* Article G01015. doi:10.1029/2011JG001818

Setiawan, Y., Yoshino, K., & Prasetyo, L. B. (2014). Characterizing the dynamics change of vegetation cover on tropical forestlands using 250 m multi-temporal MODIS EVI. *International Journal of Applied Earth Observation and Geoinformation, 26*, 132–144. doi:10.1016/j.jag.2013.06.008

Shono, K., Cadaweng, E. A., & Durst, P. B. (2007). Application of assisted natural regeneration to restore degraded tropical forestlands. *Restoration Ecology, 15*, 620–626. doi:10.1111/j.1526-100X.2007.00274.x

Sjöström, M., Ardö, J., Arneth, A., Boulain, N., Cappelaere, B., Eklundh, L., …Veenendaal, E. M. (2011). Exploring the potential of MODIS EVI for modeling gross primary production across African ecosystems. *Remote Sensing of Environment, 115,* 1081–1089. doi:10.1016/j.rse.2010.12.013

Ssekuubwa, E., van Goor, W., Snoep, M., Riemer, K., Wanyama, F., & Tweheyo, M. (2021). Recovery of seedling community attributes during passive restoration of a tropical moist forest in Uganda. *Applied Vegetation Science, 24,* e12559. doi:10.1111/avsc.12559

Steininger, M. K. (1996). Tropical secondary forest regrowth in the Amazon: age, area and change estimation with Thematic Mapper data. *International Journal of Remote Sensing, 17*, 9–27. doi:10.1080/01431169608948984

Struhsaker, T. T. (1997). *Ecology of an African rain forest: Logging in Kibale and the conflict between conservation and exploitation*. Gainesville, FL: University Press of Florida.

Sun, W., Song, X., Mu, X., Gao, P., Wang, F., & Zhao, G. (2015). Spatiotemporal vegetation cover variations associated with climate change and ecological restoration in the Loess Plateau. *Agricultural and Forest Meteorology, 209-210*, 87–99. doi:10.1016/j.agrformet.2015.05.002

Tucker, C. J. (1979). Red and photographic infrared linear combinations for monitoring vegetation. *Remote Sensing of Environment, 8,* 127–150. doi:10.1016/0034-4257(79)90013-0

Tucker, C. J., Townshend, J. R. G., & Goff, T. E. (1985). African land-cover classification using satellite data. *Science, 227,* 369–375. doi:10.1126/science.227.4685.369

UN. (2021). United Nations Decade on Ecosystem Restoration 2021-2030. Retrieved from https://www.decadeonrestoration.org/

USGS. (2020). MOD13Q1 v006. MODIS/Terra Vegetation Indices 16-Day L3 Global 250 m SIN Grid. Retrieved from https://lpdaac.usgs.gov/products/mod13q1v006/

UWA-FACE. (2015). Natural high forest rehabilitation project on degraded land of Kibale National Park, Uganda. CCB Project Design Document. UWA & Face the Future. Retrieved from https://www.climate-standards.org/2015/04/20/natural-high-forest-rehabilitation-project-on-degraded-land-of-kibale-national-park-uganda/

Valtonen, A., Molleman, F., Chapman, C. A., Carey, J. R., Ayres, M. P., & Roininen, H. (2013). Tropical phenology: bi-annual rhythms and interannual variation in an Afrotropical butterfly assemblage. *Ecosphere, 4,* Article 36. doi:10.1890/ES12-00338.1

Verbesselt, J., Hyndman, R., Newnham, G., & Culvenor, D. (2010). Detecting trend and seasonal changes in satellite image time series. *Remote Sensing of Environment, 114*, 106-115. doi:10.1016/j.rse.2009.08.014

Verbesselt, J., Umlauf, N., Hirota, M., Holmgren, M., Van Nes, E. H., Herold, M., Zeileis, A., & Scheffer, M. (2016). Remotely sensed resilience of tropical forests. *Nature Climate Change, 6*, 1028–1031. doi:10:1038/NCLIMATE3108

Viani, R. A. G., Holl, K. D., Padovezi, A., Strassburg, B. B. N., Farah, F. T., Garcia, L. C., … Brancalion, P. H. S. (2017). Protocol for monitoring tropical forest restoration: Perspectives from the Atlantic Forest restoration pact in Brazil. *Tropical Conservation Science, 10*, 1–8. doi:10.1177/1940082917697265

Vijith, H., & Dodge-Wan, D. (2020). Applicability of MODIS land cover and Enhanced Vegetation Index (EVI) for the assessment of spatial and temporal changes in strength of vegetation in tropical rainforest region of Borneo. *Remote Sensing Applications: Society and Environment, 18*, Article 100311. doi:10.1016/j.rsase.2020.100311

Wang, F., Pan, X., Gerlein-Safdi, C., Cao, X., Wang, S., Gu, L., Wang, D., & Lu, Q. (2020) Vegetation restoration in Northern China: A contrasted picture. *Land Degradation & Development, 31*, 669–676. doi:10.1002/ldr.3314

Wanyama, D., Moore N. J., & Dahlin, K. M. (2020). Persistent vegetation greening and browning trends related to natural and human activities in the Mount Elgon ecosystem. *Remote Sensing, 12*, Article 2113. doi:10.3390/rs12132113

Wheeler, C. E., Omeja, P. A., Chapman, C. A., Glipin, M., Tumwesigye, C., & Lewis, S. L. (2016). Carbon sequestration and biodiversity following 18 years of active tropical forest restoration. *Forest Ecology and Management, 373*, 44–55. doi:10.1016/j.foreco.2016.04.025

Wing, L., & Buss, I. (1970). Elephants and Forests. *Wildlife Monographs,* (19), 3–92. Retrieved from http://www.jstor.org/stable/3830398

Wu, Z., Yu, L., Zhang, X., Du, Z., & Zhang, H. (2019). Satellite-based large-scale vegetation dynamics in ecological restoration programmes of Northern China. *International Journal of Remote Sensing, 40*, 2296–2312. doi:10.1080/01431161.2018.1519286

Xiao, X., Hagen, S., Zhang, Q., Keller, M., & Moore, B. (2006). Detecting leaf phenology of seasonally moist tropical forests in South America with multi-temporal MODIS images. *Remote Sensing of Environment, 103*, 465–473. doi:10.1016/j.rse.2006.04.013

Zahawi, R. A., Dandois, J. P., Holl, K. D., Nadwodny, D., Reid, J. L., & Ellis, E. C. (2015). Using lightweight unmanned aerial vehicles to monitor tropical forest recovery. *Biological Conservation, 186,* 287–295. doi:10.1016/j.biocon.2015.03.031

Zhang, Y., Peng, C., Li, W., Tian, L., Zhu, Q., Chen, H., … Xiao, X. (2016). Multiple afforestation programs accelerate the greenness in the 'Three North' region of China from 1982 to 2013. *Ecological Indicators, 61*, 404–412. doi:10.1016/j.ecolind.2015.09.041

Zuur, A. F., Ieno, E. N., Walker, N. J., Saveliev, A. A., & Smith, G. M. (2009). *Mixed effects models and extensions in ecology with R*. New York, NY: Springer.

Supplementary Material

This manuscript contains Supplementary Material file entitled "valtonen_etal_SupplementaryMaterial.docx"

Figure legends

Figure 1. Map of the study area in Kibale National Park, Uganda. Symbols show the 2,853 grids selected for analyses (a more detailed map showing areas with planting years in Figure S2, Supplementary Material). Map generated with QGIS version 3.14.

Figure 2. Mean (±SE) NDVI (A.) and EVI (B.) in 2020, for each forest age, i.e., years since restoration started (the quadratic models are shown on top). Grids representing passive restoration were given forest age 25 years. The mean of the primary forest is shown as a dotted horizontal line.

Figure 3. Mean monthly NDVI (A.) and EVI (B.) in the seven management classes. The vertical bars show mean monthly precipitation (sources in Figure S4, Supplementary Material).

Figure 4. Mean NDVI and EVI in 2013, and ground-measured stand basal area of trees DBH ≥ 5 cm (A-B.), shrub cover (C-D.), and elephant grass cover (E-F.) across the 146 grids. If statistically significant, estimated smoothing curves (cubic regression splines) and point-wise 95% confidence bands from Generalized Additive Models are shown on top.

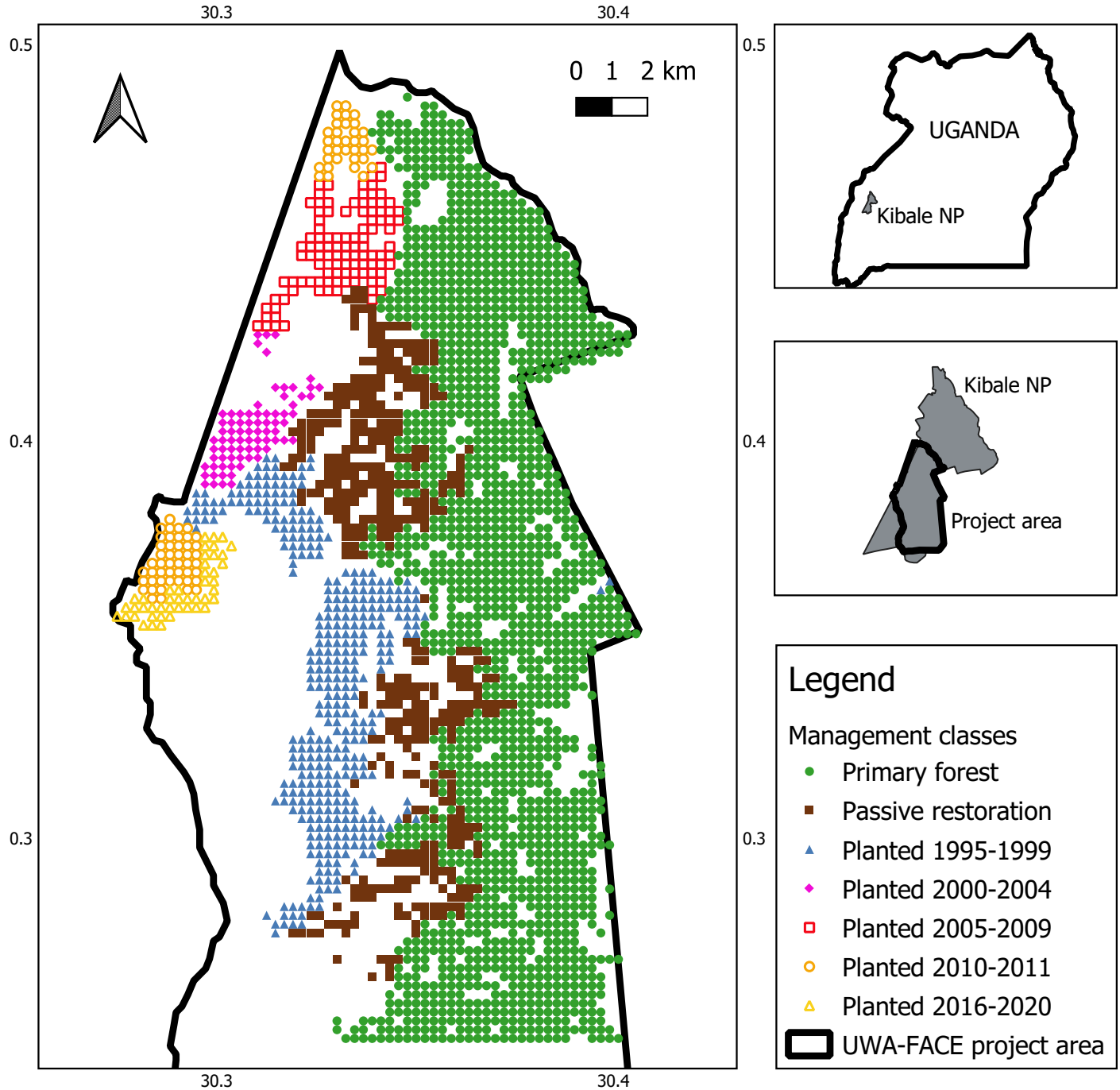
30.3
30.4
0.5
0.4
0.3
0 1 2 km
UGANDA
Kibale NP
Kibale NP
Project area
Legend
Management classes
Primary forest
Passive restoration
Planted 1995-1999
Planted 2000-2004
Planted 2005-2009
Planted 2010-2011
Planted 2016-2020
UWA-FACE project area

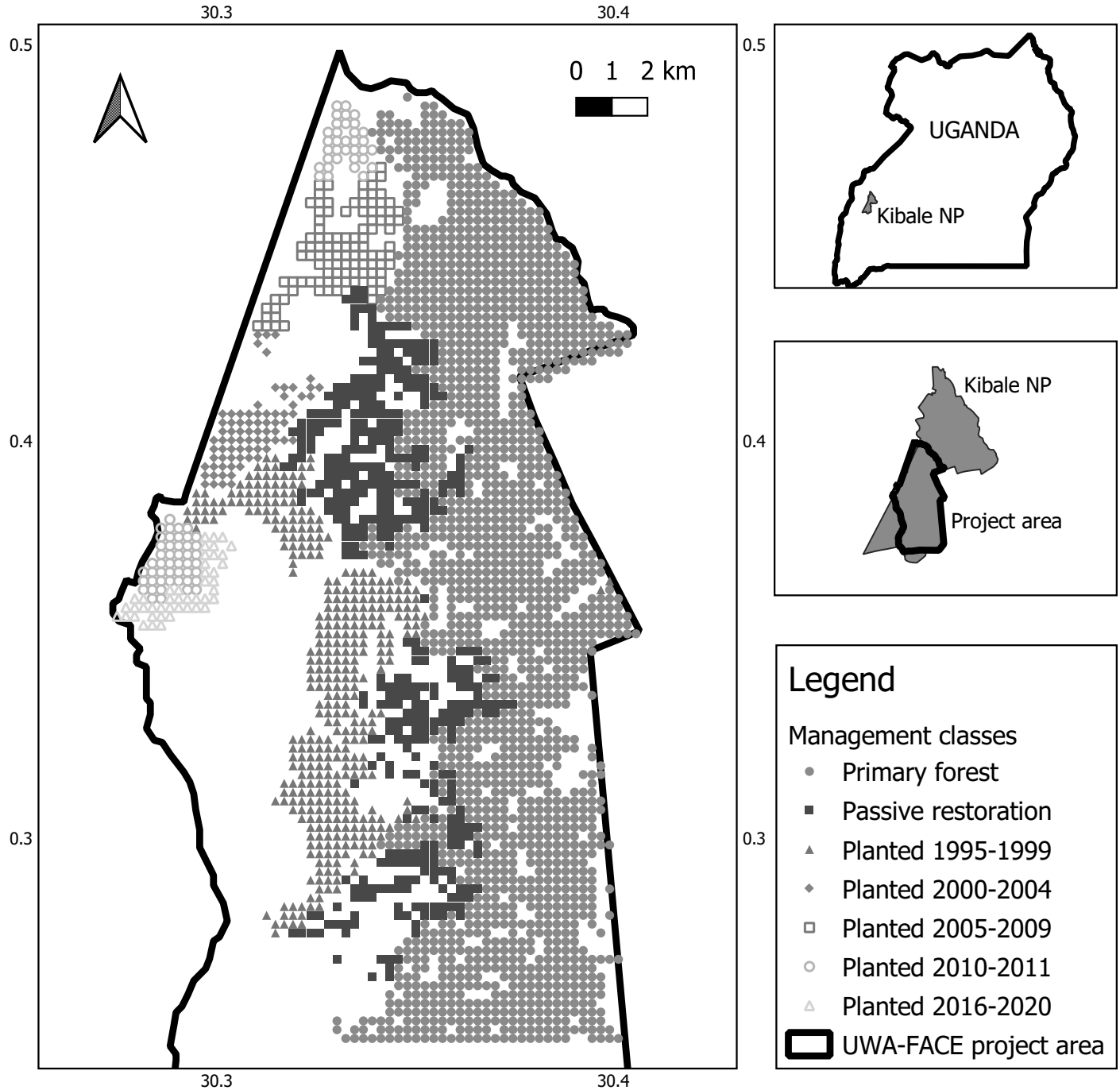
30.3
30.4
0.5
0.4
0.3
0 1 2 km
UGANDA
Kibale NP
Kibale NP
Project area
Legend
Management classes
Primary forest
Passive restoration
Planted 1995-1999
Planted 2000-2004
Planted 2005-2009
Planted 2010-2011
Planted 2016-2020
UWA-FACE project area